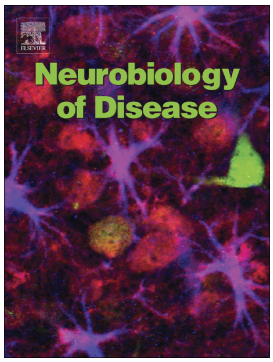

A novel de novo HCN1 loss-of-function mutation in genetic generalized epilepsy causing increased neuronal excitability

Mattia Bonzanni, Jacopo C. DiFrancesco, Raffaella Milanesi, Giulia Campostrini, Barbara Castellotti, Annalisa Bucchi, Mirko Baruscotti, Carlo Ferrarese, Silvana Franceschetti, Laura Canafoglia, Francesca Ragona, Elena Freri, Angelo Labate, Antonio Gambardella, Cinzia Costa, Ilaria Rivolta, Cinzia Gellera, Tiziana Granata, Andrea Barbuti, Dario DiFrancesco

PII:	S0969-9961(18)30191-8
DOI:	doi:10.1016/j.nbd.2018.06.012
Reference:	YNBDI 4200
To appear in:	*Neurobiology of Disease*
Received date:	2 February 2018
Revised date:	11 June 2018
Accepted date:	15 June 2018

Please cite this article as: Mattia Bonzanni, Jacopo C. DiFrancesco, Raffaella Milanesi, Giulia Campostrini, Barbara Castellotti, Annalisa Bucchi, Mirko Baruscotti, Carlo Ferrarese, Silvana Franceschetti, Laura Canafoglia, Francesca Ragona, Elena Freri, Angelo Labate, Antonio Gambardella, Cinzia Costa, Ilaria Rivolta, Cinzia Gellera, Tiziana Granata, Andrea Barbuti, Dario DiFrancesco , A novel de novo HCN1 loss-of-function mutation in genetic generalized epilepsy causing increased neuronal excitability. Ynbdi (2018), doi:10.1016/j.nbd.2018.06.012

A novel *de novo HCN1* loss-of-function mutation in genetic generalized epilepsy causing increased neuronal excitability

Mattia Bonzanni*[1], Jacopo C. DiFrancesco*#[2,3], Raffaella Milanesi[1], Giulia Campostrini[1], Barbara Castellotti[4], Annalisa Bucchi[1], Mirko Baruscotti[1], Carlo Ferrarese[3], Silvana Franceschetti[2], Laura Canafoglia[2], Francesca Ragona[5], Elena Freri[5], Angelo Labate[6], Antonio Gambardella[6], Cinzia Costa[7], Ilaria Rivolta[8], Cinzia Gellera[4], Tiziana Granata[5], Andrea Barbuti#[1], Dario DiFrancesco[1].

*These authors contributed equally

1. Dept. of Biosciences, The PaceLab, University of Milano, Milano, Italy
2. Clinical Neurophysiology and Epilepsy Center, "C. Besta" Neurological Institute, Milano, Italy.
3. Dept. of Neurology, San Gerardo Hospital, Laboratory of Neurobiology, Milan Center for Neuroscience, University of Milano-Bicocca, Monza, Italy
4. Unit of Genetics of Neurodegenerative and Metabolic Diseases, "C. Besta" Neurological Institute, Milano, Italy
5. Dept. of Pediatric Neuroscience, "C. Besta" Neurological Institute, Milano, Italy
6. Institute of Neurology, University "Magna Graecia", Catanzaro, Italy
7. Neurology Unit, Department of Medicine, University of Perugia, Ospedale S. Maria della Misericordia, Perugia, Italy
8. School of Medicine and Surgery, Milan Center for Neuroscience and Nanomedicine Center, University of Milano-Bicocca, Monza, Italy

Correspondence to:
-Barbuti A., Department of Biosciences, University of Milano, via Celoria 26, 20133 Milano, Italy, andrea.barbuti@unimi.it
-DiFrancesco J.C., Department of Neurophysiology, "C. Besta" Neurological Institute, Milan, Italy; Department of Neurology, San Gerardo Hospital and Laboratory of Neurobiology, Milan Center for Neuroscience, University of Milano-Bicocca, 20052 Monza, Italy, jacopo.difrancesco@gmail.com - jacopo.difrancesco@unimib.it

Running title: *de novo HCN1* mutation in GGE

Keywords: HCN1, genetic generalized epilepsy, electrophysiology, membrane excitability

1. ABSTRACT

The causes of genetic epilepsies are unknown in the majority of patients. HCN ion channels have a widespread expression in neurons and increasing evidence demonstrates their functional involvement in human epilepsies. Among the four known isoforms, HCN1 is the most expressed in the neocortex and hippocampus and *de novo HCN1* point mutations have been recently associated with early infantile epileptic encephalopathy. So far, HCN1 mutations have not been reported in patients with idiopathic epilepsy. Using a Next Generation Sequencing approach, we identified the de novo heterozygous p.Leu157Val (c.469C>G) novel mutation in HCN1 in an adult male patient affected by genetic generalized epilepsy (GGE), with normal cognitive development. Electrophysiological analysis in heterologous expression model (CHO cells) and in neurons revealed that L157V is a loss-of-function, dominant negative mutation causing reduced HCN1 contribution to net inward current and responsible for an increased neuronal firing rate and excitability, potentially predisposing to epilepsy. These data represent the first evidence that autosomal dominant missense mutations of *HCN1* can also be involved in GGE, without the characteristics of epileptic encephalopathy reported previously. It will be important to include *HCN1* screening in patients with GGE, in order to extend the knowledge of the genetic causes of idiopathic epilepsies, thus paving the way for the identification of innovative therapeutic strategies.

2. INTRODUCTION

Although the genetic causes of epilepsy remain unknown in most patients, significant progress in the understanding of the pathogenic mechanisms underlying the disease has been recently achieved, based on the advancement of specific diagnostic tools. Thanks to the development of the Next Generation Sequencing (NGS) techniques, the number of genes recognized to contribute, when defective as a consequence of a mutation, to different forms of epilepsy has grown substantially. This has allowed to clarify the basis of some of the specific mechanisms leading to the epileptic phenotype and, more importantly, has laid the basis for the development of innovative therapeutic approaches based on the mutations identified (Thomas & Berkovic, 2014).

Recently, the genetic causes of epilepsies with infantile/childhood-onset associated with developmental delay, such as the epileptic encephalopathies, have been identified in an increasing number of cases. Specific ion channel mutations, modifying the channel properties and affecting neuronal discharge in a way that may help development of epilepsy, have been identified in these patients (Thomas & Berkovic, 2014).

Conversely, in the case of epilepsy without cognitive impairment, such as genetic generalized epilepsy (GGE), the genetic basis is still unresolved, although many cases have a clear familial transmission, often with autosomal dominant inheritance. Studies of large cohorts of patients, with both sporadic and familial cases, have shown that a clearly identifiable genetic etiology of the disease is lacking in most cases (Heinzen *et al.*, 2012). The generally accepted view is that idiopathic epilepsies are likely determined by a complex interaction between genetic and environmental factors predisposing patients to the development of a specific phenotype (Heinzen *et al.*, 2012; Leu *et al.*, 2012). However, the complex dynamics regulating these mechanisms are far from being clarified.

Along with the ion channels already known to play a role in epilepsy, a novel group of proteins recently proposed to play a role in the pathogenesis of epilepsy is the family of the Hyperpolarization-activated, Cyclic-Nucleotide-gated (HCN) channels. The four isoforms (HCN1-4) of this family are the molecular correlates of native hyperpolarization-activated f channels carrying the "funny" current in cardiomyocytes and the "h" current in neurons (I_f/I_h).

One of the most specific functions of HCN is their involvement in generation and modulation of rhythmic activity, which is typified by the role they play in the spontaneous activity and frequency control of pacemaker cells of the heart (Brown *et al.*, 1979; DiFrancesco, 1993).
In the CNS, the HCN1, HCN2 and HCN4 isoforms are widely distributed and contribute to the generation of neuronal activity, while the role of HCN3 is less well determined (Biel *et al.*, 2009).
Neuronal HCN channels are responsible for several important cellular functions, including the contribution to cellular excitability and plasticity phenomena in the brain.
The role of HCN channels in the control of neuronal excitability and firing has been demonstrated in several types of neurons (Robinson & Siegelbaum, 2003; Biel *et al.*, 2009), which directly implies a potential involvement in pathological manifestations of neuronal activity such as epilepsy (Baruscotti *et al.*, 2010; Albertson *et al.*, 2013; Benarroch, 2013; Shah *et al.*, 2013).
Growing evidence for a relevant role of HCN channels in the pathogenesis of epilepsy has in fact emerged in the last few years (DiFrancesco & DiFrancesco, 2015; Oyrer *et al.*, 2018). Data from animal models show that the loss of HCN1 increases the dendritic input resistance in cortical neurons, leading to greater synaptic integration and firing and thus predisposing to hyperexcitability, without however generating spontaneous seizures (Huang *et al.*, 2009; Santoro *et al.*, 2010). HCN2 knockout animal models exhibit spontaneous absence seizures (Ludwig *et al.*, 2003), and generalized epileptic activity has been shown in a spontaneous mutation leading to truncation of the *HCN2* channel at the C terminus (Chung *et al.*, 2009). Moreover, pharmacological animal models of epilepsy show a remodeling of HCN channels following the induction of status epilepticus, leading to an enduring predisposition to spontaneous seizures (Jung *et al.*, 2007; Powell *et al.*, 2008; Jung *et al.*, 2011).
In patients, evidence is accumulating for HCN mutations associated with epileptic phenotypes, although the data are still not sufficient to draw a general paradigm linking HCN properties and epilepsy.
The first study exploring the presence of HCN mutations in patients with generalized epilepsy identified a single point mutation in the C-linker region of *HCN2*, leading to a partial reduction of activity of the mutant channel (Tang *et al.*, 2008). Dibbens and colleagues later reported a gain of function mutation of *HCN2*, due to a triple proline deletion (delPPP), with higher prevalence in children affected by either febrile seizures (FS) or genetic epilepsy with febrile seizures plus (GEFS+) than in controls (Dibbens *et al.*, 2010). A study from our group led to the identification, in a patient with generalized epilepsy, of the first epilepsy-linked recessive mutation in *HCN2* (E515K) causing an essentially complete loss of channel function, with a significant increase in the activity of neuronal discharge and excitability (DiFrancesco *et al.*, 2011). In a later study the *HCN2* p.S126L mutation was identified in two subjects with FS (Nakamura *et al.*, 2013). Functional characterization showed an increased I_h availability only at high temperatures (38°C), potentially contributing to hyperthermia-induced neuronal hyperexcitability in these subjects (Nakamura *et al.*, 2013). More recently, *de novo HCN1* mutations have been reported in early infantile epileptic encephalopathy (EIEE) (Nava *et al.*, 2014a), a severe condition of infancy resembling the spectrum of Dravet syndrome and associated in the majority of cases with mutations in *SCN1A* and *PCDH19* (Depienne *et al.*, 2009a; Depienne *et al.*, 2009b). Some of the *HCN1* mutations identified have been characterized in a CHO cell model, resulting in a dominant gain-of-function effect. Notably, *HCN1* exon deletions have been reported in autism spectrum disorder without epilepsy (Nava *et al.*, 2014b). These results suggest that mutations altering HCN1 channel function are poorly tolerated and can predispose to neuronal hyperexcitability, but this may not be enough to cause seizure development. So far, *de novo HCN1* mutations have been associated with severe EE of infancy, but there is still no clear-cut evidence for their involvement in GGE (Tang *et al.*, 2008; Dibbens *et al.*, 2010; DiFrancesco *et al.*, 2011).
In this study, we report the identification of a novel, *de novo* mutation of *HCN1* in one patient affected by GGE. Functional analysis with wild type and mutant channels transfected into CHO

cells and neurons show that this mutation determines a loss-of-function effect and increased neuronal excitability, potentially predisposing the proband to the development of the disease.

2. Materials and methods

2.1. Patient recruitment

We recruited patients with the diagnosis of genetic generalized epilepsy (GGE) and focal epilepsy of unknown origin according to definition (Berg *et al.*, 2010; Scheffer *et al.*, 2017). For all patients included, we collected information about gender, type of epilepsy (generalized, focal and combined generalized and focal) and inheritance of the disease, considering it as either sporadic, when the patient is the only affected of the family, or familial, when at least one member of the proband's family is affected by epilepsy with similar features. In order to identify a possible symptomatic etiology of seizures, clinical and instrumental data of patients with epilepsy were carefully analyzed. Structural causes of seizures, such as cerebrovascular disease, tumor or trauma, were investigated with 1 or 1.5 T brain MRI with proper sequences (T1, T1 with Gadolinium, T2/FLAIR, Inversion Recovery). Biochemical and hematological tests were performed to exclude metabolic causes. Other seizure-provoking factors like antipsychotic or antidepressant therapy, alcohol or drug dependency, infection of the central nervous system were excluded. EEG was used to characterize features of the disease. Subjects with symptomatic epilepsy were excluded from recruitment. A written informed consent was obtained from all patients and/or from their parents for research purposes as approved by the local Institutional Review Board of the Besta Institute and S. Gerardo Hospital and by the Italian Ministry of Health. Upon acceptance of the informed consent, patients underwent a small blood withdrawal in EDTA anticoagulant for DNA extraction.

2.2. DNA extraction and genetic screening

Screening of *HCN* genes was performed on genomic DNA extracted from whole blood using standard procedures (QIAamp DNA Blood Mini Kit; Qiagen), as previously reported (DiFrancesco *et al.*, 2014; DiFrancesco *et al.*, 2015).

Mutations were identified by DNA sequencing (Bio-Fab Research). Following the identification of the novel p.Leu157Val mutation on HCN1, the DNA of the proband and both sisters was analyzed with an NGS gene panel. This analysis was conducted in order to rule out other possible causative genetic factors associated with the patient's phenotype. We used a Nextera Rapid Capture method with Studio Design software (Illumina, Inc., San Diego, CA, USA) for customizing a gene panel for the analysis of the genes reported in Table 1. The mean of coverage for this panel was 96%; the coverage of each gene is available on request. The resulting sequences have been aligned to the reference genome (GRCh37/hg19) using MiSeq software. Data analysis was obtained using the following software: Illumina MiSeq Reporter *vs* 2.4.60, Illumina Variant Studio *vs* 2.2, Qiagen CLC Genomics Workbench *vs* 7.0. Variants with MAF>1% reported in the dbSNP (https://www.ncbi.nlm.nih.gov/projects/SNP/), 1000 Genome (browser.1000genomes.org), EVS database (evs.gs.washington.edu) and ExAC database (http://exac.broadinstitute.org/) were considered benign variants and excluded from the report.

2.3.Construction of plasmids

The Wild Type (WT) HCN1 sequence was subcloned into the pIRES vector. The point mutation 469C>G (L157V) was introduced using the QuikChange II XL site-directed mutagenesis kit (Thermofischer) with the following primers: forward (5'-gatttaataatgcttataatgatggttggaaatgtagtcatcataccagttg-3'), reverse (5'-caactggtatgatgactacatttccaaccatcattataagcattattaaatc-3').

DNA-Binding Protein	*ARX, CHD2, EMX2, FOXG1,HESX1, MBD5, MECP2, MEF2C, TCF4, ZEB2*
Enzyme	*AFG3L2, ALDH7A1, CDKL5, CERS1, CSTB, CTSD, EMPM2A, GBA, KDM6A, KMT2D, MAGI2, NEU1, NHLRC1, PAFAHB1B, SMS, TPP1, EBE3A, WWOX*
Ion Channels and receptors	*ATP1A2, CACNA1A, CHRNA2, CHRNB2, CLCN2, GABRB3, GABRG2, GRIN2B, HCN1, HCN2, HCN4, KCNC1, KCNE2, KCNQ2, KCNQ3, KCNT1, KCTD7, SCN1A, SCN1B, SCN2A, SCN8A*
Structural Proteins	*ADGRG1, APBA2, CAV3, COL4A1, COL4A2, DCX, FLNA, GRASP, PCDH19, SLC2A1, SLC6A8, SLC9A6, TUBA1A, TUBB2B, TUBB3, TUBB8*
Other	*ARHGEF9, C10ORF2, CLN6, DEPDC5, GOSR2, NPC1, NPC2, PEX5L, SCARB2, SRPX2, STX1B, SYNGAP1, TBC1D24, VLDLR*

Table 1. *List of genes analyzed in the customized panel.*

2.4. Cell culture and Transfection

Chinese Hamster Ovary (CHO) cells were maintained in F-12 Ham's Medium (Euroclone) containing: 10% FBS (Gibco), 2% PenStrep Solution (Sigma), 1 mM L-Glutamine (Sigma) and 1.5 g/L $NaHCO_3$ (Sigma) at 37°C in a 5% CO_2 incubator. All animal procedures conformed to the Italian and UE laws (D. Lgs n° 2014/26, 2010/63/UE) and approved by the University of Milano Ethical Committee and by the Italian Minister of Health (protocol number 9/2013). Neonatal rat cortical neurons were isolated from 3-day old rat pups (Envigo) as previously reported (DiFrancesco *et al.*, 2011). Briefly, brains from rat pups were isolated, placed into dishes containing ice-cold dissociation medium (in mM: 134 Na-isethionic acid, 23 glucose, 15 HEPES, 2 KCl, 4 $MgCl_2$, 0.1 $CaCl_2$, and 10 kynurenic acid, pH 7.2). Cerebral cortex was dissected, chopped into small pieces and digested in the dissociation medium containing 1.3 mg/mL protease (Sigma Aldrich) for 20 minutes at 37°C. After two washes with the dissociation medium, the mechanical procedure was performed using a series of fire-polished Pasteur pipettes of decreasing size. $8x10^5$ neurons were plated onto poly-D-Lysine-coated 35 mm petri dishes containing Neuorbasal A culture medium (Invitrogen) supplemented with 1 mM Glutamax-1 (Invitrogen), B-27 (Life Technologies), 10 ng/ml β-FGF (Invitrogen), 50 U/ml penicillin G (Sigma), and 50 μg/ml streptomycin (Sigma). After the isolation procedure, rat neonatal cortical neurons presented a

limited dendritic arborization and were mostly rounded up and expressed a negligible endogenous I_h current, as previously shown (DiFrancesco et al., 2011). The medium was replaced after 1 hour in 5% CO_2 and at 37°C with Neurobasal A culture medium. Neurons were kept in 5% CO_2 at 37°C and transfected the day after isolation. Transient transfections were performed using the Lipofectamine 2000 kit (Life Technologies) for neurons and Fugene HD (Promega) for CHO cells accordingly to manufacturer instructions. For neurons, 2.5 µL of Lipofectamine was used for each 1 µg of cDNA. Lipofectamine 2000 was premixed with Serum Free Optimem in a glass tube for 5 minutes, and thereafter cDNA was added. The mixture was kept 15 minutes at room temperature, in the dark. The day after the transfection, half of the media was changed. 36-48 hours after transfection, GFP-positive neurons were selected for patch-clamp analysis. For voltage-clamp experiments, 1.5 µg of either WT hHCN1- or L157V hHCN1-containing plasmids, or plasmids containing 0.75 µg of both were transfected into either CHO cells or neurons. For current-clamp experiments, neurons were transfected with either 0.5 µg of WT hHCN1- or L157V hHCN1-containing plasmids, or with plasmids containing 0.25 µg of both.

2.5. Electrophysiology

Patch-clamp experiments in the whole-cell configuration were carried out 36-48 hours after transfection on GFP-positive cells at room temperature. CHO cells were initially superfused with the Tyrode solution (mM: 140 NaCl, 5.4 KCl, 1.8 $CaCl_2$, 1 $MgCl_2$, 5.5 D-glucose, 5 Hepes-NaOH; pH 7.4). To dissect I_{HCN1}, cells were superfused with a high potassium solution containing (mM): 110 NaCl, 0.5 $MgCl_2$, 1.8 $CaCl_2$, 5 Hepes-NaOH, 30 KCl, 1 $BaCl_2$, 2 $MnCl_2$, pH 7.4. Patch-clamp pipettes had a resistance of 5-7 MΩ when filled with the intracellular-like solution containing (mM): 130 KCl, 10 NaCl, 1 EGTA-KOH, 0.5 MgCl2, 2 ATP (Na-salt), 5 creatine phosphate, 0.1 GTP, 5 Hepes-KOH; pH 7.2. Neurons were superfused with an external solution containing (mM): 129 NaCl, 1.25 NaH_2PO_4, 1.8 $MgSO_4$, 1.6 $CaCl_2$, 3 KCl, 10 Na-HEPES, 35 glucose, pH 7.4. The pipette solution was composed by (mM): 120 K-gluconate, 15 KCl, 2 MgCl2, 0.2 EGTA, 20 phosphocreatine, 2 ATP-disodium, 0.2 GTP-disodium, 0.1 leupeptin, 10 HEPES-KOH, pH 7.2. I_{HCN1} activation curves were obtained with a standard protocol consisting of test steps from a holding potential of -30 mV to the range -35/-115 mV, of a duration sufficient to reach steady-state activation at each voltage, followed by a fully-activating step to -125 mV in CHO cells or -115 mV in neurons.

Activation curves were fitted using the Boltzmann distribution: $y=1/(1+\exp((V-V_{1/2})/s))$, where V is voltage, y the fractional activation, $V_{1/2}$ the half-activation voltage, and s the inverse-slope factor.

I_{HCN1} activation time constants were obtained by fitting the current traces obtained from the activation protocol to a mono-exponential function. Deactivation time constants were similarly obtained in CHO cells by fitting deactivating current traces recorded at voltages in the range -75/25 mV after a fully activating step at -125 mV.

Patch-clamp currents were acquired with a sampling rate of 2 KHz and lowpass filter of 0.2 kHz. Currents were normalized to cell capacitance. Neither series resistance compensation nor leak correction were applied. In current clamp experiments, neurons were held at -70 mV; the input resistance was measured in each cell prior to starting clamp protocols and low input resistance cells (<150 MΩ) were discarded.

To investigate neuronal excitability, 2500 ms depolarizing current steps were applied in current clamp mode in 10 pA increments from the resting potential held at -70 mV, and the firing rate was measured during the first 500 ms of current step. Spike threshold was defined, for each neuron, as the first current step able to induce action potential firing.

Voltage "sags" were measured in response to 350 pA hyperpolarizing current steps of 800 ms duration. We used the equation: Sag ratio= $(V_{peak}-V_{ss})/V_{peak}$ where V_{peak} is the maximum voltage deflection and V_{ss} is the steady-state voltage at the end of the hyperpolarizing pulse (George *et al.*,

2009). All protocols were designed using Pclamp 10.2 (Axon) and data were analyzed using Origin Pro 9 (Origin Lab).

2.6. Statistical Analysis

Data were analyzed with Clampfit (Axon) and Origin Pro 9. Activation curves were compared by analyzing the $V_{1/2}$ using One-Way ANOVA followed by Fisher's LSD post-hoc test; significance level was set to $p=0.05$. Data outliers were excluded using Tukey's method. Data were collected from at least 3 different transfection experiments or primary cultures.

3. RESULTS

3.1. Genetic screening

We recruited 136 patients affected by GGE (103), focal (31) and combined generalized and focal epilepsies (2) for the genetic screening of HCN channels. In one male patient, we identified the novel variant p.Leu157Val (c.469C>G) on exon 2 of *HCN1* in heterozygosis. The extension of the analysis to the family of the proband (parents and siblings) revealed that this was a *de novo* variant in the proband (Fig. 1A). NGS analysis did not reveal other significant epilepsy-related genetic variants potentially linked to the phenotype of the proband. Residue Leu157 of hHCN1 is localized about midway of the first transmembrane domain (S1) of the hHCN1 channel core (Fig 1C) and is conserved through all HCN isoforms (Fig. 1D).

Figure 1. *A, pedigree of the family investigated. Red indicates the generalized epilepsy phenotype (proband). The crossed symbol represents expression of heterozygous L157V mutation in HCN1. The mutation is missing in either parents of the proband and is therefore a* de novo *mutation. B, EEG of the proband showing generalized sharp waves. C, top, diagram of a single HCN1 subunit showing the approximate position of residue Leu157. C, bottom, 3D ribbon representation of the structure of hHCN1, based on Cryo-EM reconstruction (Lee & MacKinnon 2017, PDB ID: 5U6P). Shown are two of the 4 subunits, including core transmembrane domains (green and orange), HCN domains (blue) and C-termini (red). L157V mutated residues in S1 domains are drawn as space-filling plots. D, sequence alignment of the S1 and S2 domains of the four hHCN isoforms, indicating the sequence location of the conserved leucine residue in S1 (hHCN1 L157, red background).*

3.2. Case description

The patient carrying the novel variant p.Leu157Val (c.469C>G) on *HCN1* was born from a physiological pregnancy, by non-consanguineous parents. He presented a single febrile seizure at the age of 2 years. At the age of 19, he reported frequent episodes in cluster of limbs myoclonus, especially at wakeup. He started treatment with low-doses of valproate, with good control of the episodes. One year later, the patient presented tonic-clonic generalized seizures with EEG showing generalized sharp-waves, prevalent on the bilateral anterior regions (Fig. 1B). Seizure control was obtained increasing the dose of valproate treatment and this therapy has been continued until present. Brain MRI was normal and a battery of cognitive tests showed a cognitive level within normal limits.

The proband has a family history of epilepsy. The mother presented a single febrile seizure in infancy, with no history of subsequent epilepsy. Both sisters of the proband presented typical absence epilepsy in infancy, with complete resolution in childhood. The clinical picture of the proband is clearly distinct from that of his relatives.

3.3 Functional characterization of L157V HCN1 mutation in CHO cells and cortical neurons

In order to assess the biophysical properties of L157V mutant hHCN1 channels, we performed electrophysiological analysis of CHO cells transfected with wild-type and/or mutant channels.

Figure 2. *Comparison of biophysical properties of homomeric/heteromeric L157V mutant vs wild-type hHCN1 channels expressed in CHO cells. A, representative current density traces recorded in the range -45/-125 mV (-20 mV steps; holding potential -30 mV) in CHO cells expressing WT (n=14), homomeric L157V (n=17) and heteromeric WT/L157V (n=11) mutant channels, as indicated. B-D, graphs showing mean steady-state current density-voltage relations (B), activation curves (C) and time constants of activation and deactivation (D) for the 3 types of channels (symbols as in A).*

Typical traces of normalized I_{HCN1} currents recorded from cells transfected with WT, L157V homomeric channels or heteromeric WT/L157V channels are shown in Fig. 2A (left to right). Plotting mean current-voltage relations in Fig. 2B shows that both L157V and WT/L157V mutant channels carry about half of the current carried by WT channels in the whole range of activation voltages, apparently according to a dominant effect of the mutation. Mean cell capacitance was not different among cells transfected with WT (42.1±4.9 pF, n=14), homozygous L157V (37.0±4.7 pF, n=17) or heterozygous WT/L157V channels (39.7±5.2 pF, n=11) ($p>0.05$).
L157V (n=28) and WT/L157V (n=19) mutant channel also had activation curves slightly, but significantly, shifted to more positive voltages (2.3 and 3.4 mV, respectively, Fig. 2C), as well as slightly faster activation and slower deactivation time constants (Fig. 2D) relative to WT (n=25) channels.

To verify if the changes observed were also present in a neuronal background, and to verify potential effects on neuronal activity, we expressed wild type and mutant channels in neonatal rat cortical neurons (Fig. 3).

Figure 3. *Comparison of biophysical properties of homomeric/heteromeric L157V mutant vs wild-type hHCN1 channels expressed in neonatal rat cortical neurons. A, representative current density traces recorded during activation curve protocols. Steps were applied from a holding potential of -30 mV to the test range -35/-115 mV in -20 mV steps, and were followed by a fully-activating step to -115 mV. B-D, graphs showing mean steady-state current density-voltage relations (B, WT n=5, L157V n=7, WT/L157V n=6), activation curves (C, WT n=7, L157V n=9, WT/L157V n=9) and time constants of activation (D, WT n=6, L157V n=7, WT/L157V n=7) for the 3 types of channels (symbols as in A).*

Representative normalized current traces recorded in neurons transfected with WT, L157V or WT/L157V isoforms are shown in Fig. 3A (top to bottom). Capacitances of neurons transfected with different constructs were similar. Mean values were (pF): WT 22.1±2.1 (n=22), L157V 19.0±2.1 (n=18), WT/L157V 19.2±1.5 (n=18) ($p>0.05$).

As apparent from the mean current-voltage relations in Fig. 3B, expression of mutated channels was associated with strongly reduced currents relative to WT channels. The density in mutant-transfected neurons was similarly reduced by about 80% in both L157V and WT/L157V channels, and this effect was not significantly different between homomeric and heteromeric constructs. In agreement with data in CHO cells, the activation curves of both L157V and WT/L157V channels were significantly shifted to more positive voltages by about 9 mV relative to WT channels ($P<0.01$; Fig. 3C) and time constants of activation were faster particularly near mid-activation voltages (Fig. 3D). The quantitatively similar changes of current density and kinetic properties caused by homomeric and heteromeric mutant channels again point, as observed in CHO cells, to a dominant-negative effect of the mutation.

In order to verify the net effect on excitability, due to the concomitant loss-of-function change caused by a current density reduction and gain-of-function change due to the rightward shift of the current activation, we analyzed the contribution of the different constructs to neuronal activity. by first measuring the voltage-sag induced by injecting hyperpolarizing current steps (Fig. 4) and then by investigating neuronal firing and excitability (Figures 5 and 6).

Figure 4. *Hyperpolarizing voltage sag. A, superimposition of representative traces (bottom) recorded in response to a 350 pA hyperpolarizing current step (top) in WT, homomeric L157V and heteromeric WT/L157V hHCN1-transfected neurons, as indicated. All recordings were made after setting the holding resting voltage at -70 mV. All traces were normalized to the peak of voltage sag, and the sag was calculated as the a/b ratio (a, b and voltage bar refer to the WT record). B, bar graph showing mean voltage sag ratios for the three channel types. Average values were: WT, 0.17 ± 0.02 (n=15); L157V, 0.06 ± 0.01 (n=7); WT/L157V 0.06 ± 0.03 (n=8)). *p<0.05, T-Student Test.*

In Fig. 4A, typical depolarizing sags developing in response to 350 pA hyperpolarizing current injections are shown in neurons transfected with WT, L157V or WT/L157V channels. Normalized voltage sags in neurons expressing homozygous or heterozygous mutant channels were significantly smaller (about 30%, Fig. 4B) than those in WT-expressing neurons. This indicates that the HCN1 contribution to neuronal activity is reduced by the L157V mutation, and that therefore, in the hyperpolarized range of voltages, the current density decrease prevails over the increased

contribution associated with the rightward shift of the activation curve and acceleration of activation. In accordance with a decreased contribution of the HCN1 current, neurons transfected with WT HCN1 had a resting potential significantly more depolarized than either neurons transfected with the L157V construct, both in homomeric and heteromeric conditions, or untransfected neurons (WT: -40.4±2.0 mV, n=10; L157V: -51.0±3.5, n=11; WT/L157V: -53.7±2.6, n=10; untransfected: -51.3±4.8, n=7). These data therefore suggest that L157V is a loss-of-function mutation.

3.4. Impact of L157V HCN1 mutation on neuronal excitability

In view of the known role of HCN1 channels in shaping neuronal activity (DiFrancesco & DiFrancesco, 2015; Oyrer *et al.*, 2018), and having verified that the L157V mutation affects functional properties of the HCN1 channel, we next explored if the expression of mutant channels modifies the firing properties of neurons.

Sample traces recorded from untransfected neurons and from neurons transfected with WT, L157V and WT/L157V channels during application of a depolarizing 40 pA current step of 2 s duration are shown in Fig. 5A.

Figure 5. *Impact of L157V hHCN1 mutation on firing rate. A, representative traces of AP recordings following the injection of a depolarizing 40 pA current step in untransfected neurons and in neurons expressing WT, homomeric L157V and heteromeric WT/L157V channels, as indicated. All recordings were made after setting the holding resting voltage at -70 mV, and the rate was measured during the first 500 ms of current injection. B, plot of the mean firing rates of neurons as a function of injected current (untransfected, n=5; WT, n=10; L157V, n=11; WT/L157V, n=10; symbols as in A). Lines drawn through points.*

Relative to untransfected neurons, expression of WT HCN1 channels inhibits action potential firing at relatively low values of current injected. Expression of mutant channels, however, regardless of whether in homomeric or heteromeric conditions, restores the ability of neurons to fire and re-establishes excitability. Measurement of the cell input resistance confirmed these results by showing that the input resistance was significantly reduced in neurons expressing WT channels (480.9±101.4 MΩ n=9) relative to untransfected neurons (2316.3±483.4 MΩ, n=7) or neurons expressing mutant channels (L157V: 1560.1±178.0 MΩ, n=10; WT/L157V: 1993.8±282.6 MΩ, n=10).

Extending the range of depolarizing current injection steps allows to investigate the dependence of firing rate upon stimulus intensity. This is achieved by plotting in Fig. 5B the mean firing rates calculated in the first 500 ms of current steps of increasing amplitude (from 10 to 40 pA in 10 pA steps, see Methods) applied to the 4 different conditions shown in A.

These data clearly indicate that while expression of WT HCN1 channels strongly depresses neuronal firing (action potentials could only be elicited by steps >40 pA), transfection with either homomeric or heteromeric mutant constructs returns neurons to a highly excitable state.

To further quantify changes in neuronal excitability, we also analyzed the effect of the mutation on spike threshold. Expression of mutant channels decreased the spike threshold relative to wild-type channels, as shown in Fig 6. In Fig. 6A representative records show that injection of a 150 pA depolarizing current step was required to elicit firing in neurons expressing the WT HCN1, while much lower steps (40 pA) were required to elicit a similar firing pattern in either L157V or WT/L157V –transfected neurons, and lower still in untransfected neurons.

As shown in Fig. 6B, the mean spike threshold was indeed much smaller in untransfected, L157V and WT/L157V-expressing neurons than in WT-expressing neurons.

Taken together, these results clearly indicate that, by reducing the HCN1 channel contribution to activity, the L157V mutation can induce, in an *in vitro* simplified model of neurons, increased excitability according to a negative-dominant effect.

Figure 6. *Impact of L157V hHCN1 mutation on spike threshold. A, representative traces of AP recordings made during injection of depolarizing current steps in untransfected neurons and in neurons expressing WT, homomeric L157V and heteromeric WT/L157V channels, as indicated. B, bar graph showing mean spike threshold values in untransfected neurons and in neurons expressing the three different channel types. Mean ± SEM values were (pA): untransfected, 21.0±4.0, n=5; WT, 138.9±47.7, n=9, L157V, 30.0±4.3, n=11; WT/L157V, 24.0±4.5, n=10). *p<0.05, T-Student Test.*

4. DISCUSSION

The genetic causes of generalized epilepsy are not known in a majority of patients, even in the cases where the transmission of the phenotype is clearly autosomal dominant. Most likely, there are several causes contributing to the phenotype, both genetic and environmental. In the last few years, extensive use of NGS has led to the identification of many genes whose alteration can play a role in epilepsy. A substantial fraction of these is represented by ion channel genes, whose dysfunctional mutations can be often shown to be associated with, if not directly causative of, the disease (Thomas & Berkovic, 2014).

In this work, by analyzing a cohort of patients with genetic epilepsy, we have identified for the first time a *de novo HCN1* mutation in heterozygosis in an adult patient affected by GGE, without features of epileptic encephalopathies. Notably, the epileptic phenotype, EEG characteristics, onset of symptoms and clinical evolution are markedly different from those previously reported in early infantile epileptic encephalopathy (EIEE) carrying various *de novo HCN1* mutations (Nava *et al.*, 2014a). EIEE patients were in fact characterized by a severe phenotype, with pharmacoresistant epilepsy and unfavorable prognosis in the short term. Moreover, the L157V mutation is novel and has not been reported in EIEE.
Recent data from cryo-EM resolution of the HCN1 channel structure (Lee & MacKinnon, 2017) show that the leucine 157 residue is located in the first transmembrane segment S1 of the core domain of the protein (Lee & MacKinnon, 2017). This location is unlikely to render L157 important as a docking site for regulatory proteins (such as for example MiRP1 or Trip8b), nor as a site for post-transcriptional modification.
Our data show that heterologous expression of the L157V mutation in CHO cells and in primary neonatal rat cortical neurons reveals a dual effect: a reduced current density and an increased degree of current activation due to modified current kinetic properties.

In details, we found that the expression of the L157V mutation, regardless whether in homomeric or heteromeric constructs, reduced significantly the amount of the membrane current relative to WT channels, according to a loss-of-function effect. At the same time, changes in kinetic properties of channels led to gain-of-function effects, characterized by a shift of the current activation curve to more positive voltages, a faster activation and a slower deactivation (this latter only observed for technical reasons in CHO cells). These modifications were again similar in homomeric and heteromeric constructs, ruling strongly in favor of a dominant negative effect of the mutation. The above effects were more pronounced in neurons than in CHO cells, possibly implying a more effective "context" dependence in homologous than in heterologous expression systems.

In order to verify if and how these changes impact neuronal excitability, we then turned to analyze potential modifications of electrical activity of neurons caused by expression of mutant channels.
We first analyzed the voltage sag response in neurons and found that, in neurons expressing either homo- or heteromeric L157V mutant channels, a reduced depolarizing "sag" was elicited in response to hyperpolarizing steps, indicating a loss-of-function effect relative to WT channels.
Also in accordance with a loss-of-function effect of the mutation, we found that the firing rate in response to depolarizing voltage steps was strongly amplified in neurons expressing mutant rather than WT HCN1 channels, an effect recorded irrespectively of whether expressed channels were homomeric L157V or heteromeric WT/L157V. Spike threshold was also correspondingly decreased in neurons expressing mutant channels.

The increased excitability of mutant-expressing neurons was quantitatively similar to that of untransfected neurons, in agreement with the notion that these neurons normally express a small Ih current (DiFrancesco *et al.*, 2011).

These results can be summarized to indicate that neurons expressing mutant channels are more excitable than WT-expressing neurons, due to a reduced amount of I_{HCN1} current. They represent the first evidence in a neuronal model that missense variants of *HCN1*, causing loss-of-function effects, determine an increase of neuronal excitability and discharge activity, potentially associated with epileptogenesis.
This is in line with previous observations that missense point mutations of *HCN1* are poorly tolerated and associated with epilepsy, while non-sense variants do not alter neuronal discharge activity (Nava *et al.*, 2014b).

Although the cellular effects we have observed are clear-cut in indicating an L157V-linked increase of neuronal excitability, the observation of the transmission of the disease within the family suggests a complex etiological pattern, where the mutation appears to be a contributing rather than a causative factor. Indeed the L157V *HCN1* mutation only partially segregates with the disease, since it has been identified as a *de novo* mutation only in the proband, whose epileptic phenotype is more severe than that of the sisters (typical absence epilepsy) and the mother (single febrile seizure in infancy, without epilepsy) who do not carry the mutation. All the siblings were analyzed with an extensive NGS investigation in order to identify any adjunctive cause potentially responsible for the disease, however with negative results. We can thus hypothesize that the L157V *HCN1* mutation importantly contributes to the phenotype of the proband, but that also other undetermined causes are likely to have a role in the disease in this family.

This study reports for the first time a *de novo* heterozygous missense mutation of *HCN1* in a patient with GGE, characterized by a dominant negative loss-of-function effect on channel contribution to activity. As for other channelopathies with variable characteristics and severity (i.e. *SCN1A* (Gambardella & Marini, 2009) and *KCNQ2* (Miceli *et al.*, 2013)), HCN channelopathies are emerging as potential key players in human epilepsy. Even though we cannot completely rule out the presence of other causative factors, the lack of any other mutation in almost eighty epilepsy-associated genes (Table 1) strengthens the hypothesis that the L157V HCN1 mutation may participate in the onset of the disease as an important predisposing factor. Our data also suggest that it may be important to perform HCN screening in subjects affected by GGE, which may help to increase the understanding of the pathogenic mechanisms leading to the development of the disease. This knowledge will be useful to identify innovative therapeutic strategies through the selective modulation of HCN channels, for the improvement of the treatment of patients.

ACKNOWLEDGMENTS
This work was supported by the Italian Ministry of Health grants GR-2010-2304834 to J.C.D. and A.Ba and GR-2016-02363337 to J.C.D.

REFERENCES

Albertson AJ, Williams SB & Hablitz JJ. (2013). Regulation of epileptiform discharges in rat neocortex by HCN channels. *J Neurophysiol* **110,** 1733-1743.

Baruscotti M, Bottelli G, Milanesi R, DiFrancesco JC & DiFrancesco D. (2010). HCN-related channelopathies. *Pflugers Arch* **460,** 405-415.

Benarroch EE. (2013). HCN channels: function and clinical implications. *Neurology* **80,** 304-310.

Berg AT, Berkovic SF, Brodie MJ, Buchhalter J, Cross JH, van Emde Boas W, Engel J, French J, Glauser TA, Mathern GW, Moshé SL, Nordli D, Plouin P & Scheffer IE. (2010). Revised terminology and concepts for organization of seizures and epilepsies: report of the ILAE Commission on Classification and Terminology, 2005-2009. *Epilepsia* **51,** 676-685.

Biel M, Wahl-Schott C, Michalakis S & Zong X. (2009). Hyperpolarization-activated cation channels: from genes to function. *Physiol Rev* **89,** 847-885.

Brown HF, DiFrancesco D & Noble SJ. (1979). How does adrenaline accelerate the heart? *Nature* **280,** 235-236.

Chung WK, Shin M, Jaramillo TC, Leibel RL, LeDuc CA, Fischer SG, Tzilianos E, Gheith AA, Lewis AS & Chetkovich DM. (2009). Absence epilepsy in apathetic, a spontaneous mutant mouse lacking the h channel subunit, HCN2. *Neurobiol Dis* **33,** 499-508.

Depienne C, Bouteiller D, Keren B, Cheuret E, Poirier K, Trouillard O, Benyahia B, Quelin C, Carpentier W, Julia S, Afenjar A, Gautier A, Rivier F, Meyer S, Berquin P, Hélias M, Py I, Rivera S, Bahi-Buisson N, Gourfinkel-An I, Cazeneuve C, Ruberg M, Brice A, Nabbout R & Leguern E. (2009a). Sporadic infantile epileptic encephalopathy caused by mutations in PCDH19 resembles Dravet syndrome but mainly affects females. *PLoS Genet* **5,** e1000381.

Depienne C, Trouillard O, Saint-Martin C, Gourfinkel-An I, Bouteiller D, Carpentier W, Keren B, Abert B, Gautier A, Baulac S, Arzimanoglou A, Cazeneuve C, Nabbout R & LeGuern E. (2009b). Spectrum of SCN1A gene mutations associated with Dravet syndrome: analysis of 333 patients. *J Med Genet* **46,** 183-191.

Dibbens LM, Reid CA, Hodgson B, Thomas EA, Phillips AM, Gazina E, Cromer BA, Clarke AL, Baram TZ, Scheffer IE, Berkovic SF & Petrou S. (2010). Augmented currents of an HCN2 variant in patients with febrile seizure syndromes. *Annals of neurology* **67,** 542-546.

DiFrancesco D. (1993). Pacemaker mechanisms in cardiac tissue. *Annu Rev Physiol* **55,** 455-472.

DiFrancesco JC, Barbuti A, Milanesi R, Coco S, Bucchi A, Bottelli G, Ferrarese C, Franceschetti S, Terragni B, Baruscotti M & DiFrancesco D. (2011). Recessive loss-of-function mutation in the pacemaker HCN2 channel causing increased neuronal excitability in a patient with idiopathic generalized epilepsy. *J Neurosci* **31,** 17327-17337.

DiFrancesco JC & DiFrancesco D. (2015). Dysfunctional HCN ion channels in neurological diseases. *Front Cell Neurosci* **6,** 174.

DiFrancesco JC, Novara F, Zuffardi O, Forlino A, Gioia R, Cossu F, Bolognesi M, Andreoni S, Saracchi E, Frigeni B, Stellato T, Tolnay M, Winkler DT, Remida P, Isimbaldi G & Ferrarese C. (2015). TREX1 C-terminal frameshift mutations in the systemic variant of retinal vasculopathy with cerebral leukodystrophy. *Neurol Sci* **36,** 323-330.

DiFrancesco JC, Sestini R, Cossu F, Bolognesi M, Sala E, Mariani S, Saracchi E, Papi L & Ferrarese C. (2014). Novel neurofibromatosis type 2 mutation presenting with status epilepticus. *Epileptic Disord* **16,** 132-137.

Gambardella A & Marini C. (2009). Clinical spectrum of SCN1A mutations. *Epilepsia* **50 Suppl 5,** 20-23.

George MS, Abbott LF & Siegelbaum SA. (2009). HCN hyperpolarization-activated cation channels inhibit EPSPs by interactions with M-type K(+) channels. *Nature neuroscience* **12,** 577-584.

Heinzen EL, Depondt C, Cavalleri GL, Ruzzo EK, Walley NM, Need AC, Ge D, He M, Cirulli ET, Zhao Q, Cronin KD, Gumbs CE, Campbell CR, Hong LK, Maia JM, Shianna KV, McCormack M, Radtke RA, O'Conner GD, Mikati MA, Gallentine WB, Husain AM, Sinha SR, Chinthapalli K, Puranam RS, McNamara JO, Ottman R, Sisodiya SM, Delanty N & Goldstein DB. (2012). Exome sequencing followed by large-scale genotyping fails to identify single rare variants of large effect in idiopathic generalized epilepsy. *Am J Hum Genet* **91,** 293-302.

Huang Z, Walker MC & Shah MM. (2009). Loss of dendritic HCN1 subunits enhances cortical excitability and epileptogenesis. *J Neurosci* **29,** 10979-10988.

Jung S, Jones TD, Lugo JN, Sheerin AH, Miller JW, D'Ambrosio R, Anderson AE & Poolos NP. (2007). Progressive dendritic HCN channelopathy during epileptogenesis in the rat pilocarpine model of epilepsy. *J Neurosci* **27,** 13012-13021.

Jung S, Warner LN, Pitsch J, Becker AJ & Poolos NP. (2011). Rapid loss of dendritic HCN channel expression in hippocampal pyramidal neurons following status epilepticus. *J Neurosci* **31,** 14291-14295.

Lee CH & MacKinnon R. (2017). Structures of the Human HCN1 Hyperpolarization-Activated Channel. *Cell* **168,** 111-120 e111.

Leu C, de Kovel CG, Zara F, Striano P, Pezzella M, Robbiano A, Bianchi A, Bisulli F, Coppola A, Giallonardo AT, Beccaria F, Trenité DK, Lindhout D, Gaus V, Schmitz B, Janz D, Weber YG, Becker F, Lerche H, Kleefuss-Lie AA, Hallman K, Kunz WS, Elger CE, Muhle H, Stephani U, Møller RS, Hjalgrim H, Mullen S, Scheffer IE, Berkovic SF, Everett KV, Gardiner MR, Marini C, Guerrini R, Lehesjoki AE, Siren A, Nabbout R, Baulac S, Leguern E, Serratosa JM, Rosenow F, Feucht M, Unterberger I, Covanis A, Suls A, Weckhuysen S, Kaneva R, Caglayan H, Turkdogan D, Baykan B, Bebek N, Ozbek U, Hempelmann A, Schulz H, Rüschendorf F, Trucks H, Nürnberg P, Avanzini G, Koeleman BP, Sander T & Consortium E. (2012). Genome-wide linkage meta-analysis identifies susceptibility loci at 2q34 and 13q31.3 for genetic generalized epilepsies. *Epilepsia* **53,** 308-318.

Ludwig A, Budde T, Stieber J, Moosmang S, Wahl C, Holthoff K, Langebartels A, Wotjak C, Munsch T, Zong X, Feil S, Feil R, Lancel M, Chien KR, Konnerth A, Pape HC, Biel M &

Hofmann F. (2003). Absence epilepsy and sinus dysrhythmia in mice lacking the pacemaker channel HCN2. *EMBO J* **22,** 216-224.

Miceli F, Soldovieri MV, Ambrosino P, Barrese V, Migliore M, Cilio MR & Taglialatela M. (2013). Genotype-phenotype correlations in neonatal epilepsies caused by mutations in the voltage sensor of K(v)7.2 potassium channel subunits. *Proc Natl Acad Sci U S A* **110,** 4386-4391.

Nakamura Y, Shi X, Numata T, Mori Y, Inoue R, Lossin C, Baram TZ & Hirose S. (2013). Novel HCN2 Mutation Contributes to Febrile Seizures by Shifting the Channel's Kinetics in a Temperature-Dependent Manner. *PloS one* **8,** e80376.

Nava C, Dalle C, Rastetter A, Striano P, de Kovel CG, Nabbout R, Cancès C, Ville D, Brilstra EH, Gobbi G, Raffo E, Bouteiller D, Marie Y, Trouillard O, Robbiano A, Keren B, Agher D, Roze E, Lesage S, Nicolas A, Brice A, Baulac M, Vogt C, El Hajj N, Schneider E, Suls A, Weckhuysen S, Gormley P, Lehesjoki AE, De Jonghe P, Helbig I, Baulac S, Zara F, Koeleman BP, Haaf T, LeGuern E, Depienne C & Consortium ER. (2014a). De novo mutations in HCN1 cause early infantile epileptic encephalopathy. *Nat Genet* **46,** 640-645.

Nava C, Keren B, Mignot C, Rastetter A, Chantot-Bastaraud S, Faudet A, Fonteneau E, Amiet C, Laurent C, Jacquette A, Whalen S, Afenjar A, Périsse D, Doummar D, Dorison N, Leboyer M, Siffroi JP, Cohen D, Brice A, Héron D & Depienne C. (2014b). Prospective diagnostic analysis of copy number variants using SNP microarrays in individuals with autism spectrum disorders. *Eur J Hum Genet* **22,** 71-78.

Oyrer J, Maljevic S, Scheffer IE, Berkovic SF, Petrou S, Reid CA. (2018). Ion channels in genetic epilepsy: from genes and mechanisms to disease-targeted therapies. *Pharmacol Rev* **70**, 142-173.

Powell KL, Ng C, O'Brien TJ, Xu SH, Williams DA, Foote SJ & Reid CA. (2008). Decreases in HCN mRNA expression in the hippocampus after kindling and status epilepticus in adult rats. *Epilepsia* **49,** 1686-1695.

Robinson RB & Siegelbaum SA. (2003). Hyperpolarization-activated cation currents: from molecules to physiological function. *Annu Rev Physiol* **65,** 453-480.

Santoro B, Lee JY, Englot DJ, Gildersleeve S, Piskorowski RA, Siegelbaum SA, Winawer MR & Blumenfeld H. (2010). Increased seizure severity and seizure-related death in mice lacking HCN1 channels. *Epilepsia* **51,** 1624-1627.

Scheffer IE, Berkovic S, Capovilla G, Connolly MB, French J, Guilhoto L, Hirsch E, Jain S, Mathern GW, Moshé SL, Nordli DR, Perucca E, Tomson T, Wiebe S, Zhang YH & Zuberi SM. (2017). ILAE classification of the epilepsies: Position paper of the ILAE Commission for Classification and Terminology. *Epilepsia* **58,** 512-521.

Shah MM, Huang Z & Martinello K. (2013). HCN and KV7 (M-) channels as targets for epilepsy treatment. *Neuropharmacology* **69,** 75-81.

Tang B, Sander T, Craven KB, Hempelmann A & Escayg A. (2008). Mutation analysis of the hyperpolarization-activated cyclic nucleotide-gated channels HCN1 and HCN2 in idiopathic generalized epilepsy. *Neurobiol Dis* **29,** 59-70.

Thomas RH & Berkovic SF. (2014). The hidden genetics of epilepsy-a clinically important new paradigm. *Nat Rev Neurol* **10,** 283-292.

Highlights

- We have identified a new heterozygous *de novo* mutation of *HCN1* (c.469C>G, p.L157V) in a patient affected by genetic generalized epilepsy (IGE).
- Electrophysiological analysis in CHO cell and in neonatal neurons has revealed that L157V reduces, in a dominant-negative manner, the HCN1 current.
- When expressed in neurons, mutant channels reduce the firing threshold and increase excitability.
- This is the first evidence that loss-of-function HCN1 mutations can predispose to GGE.

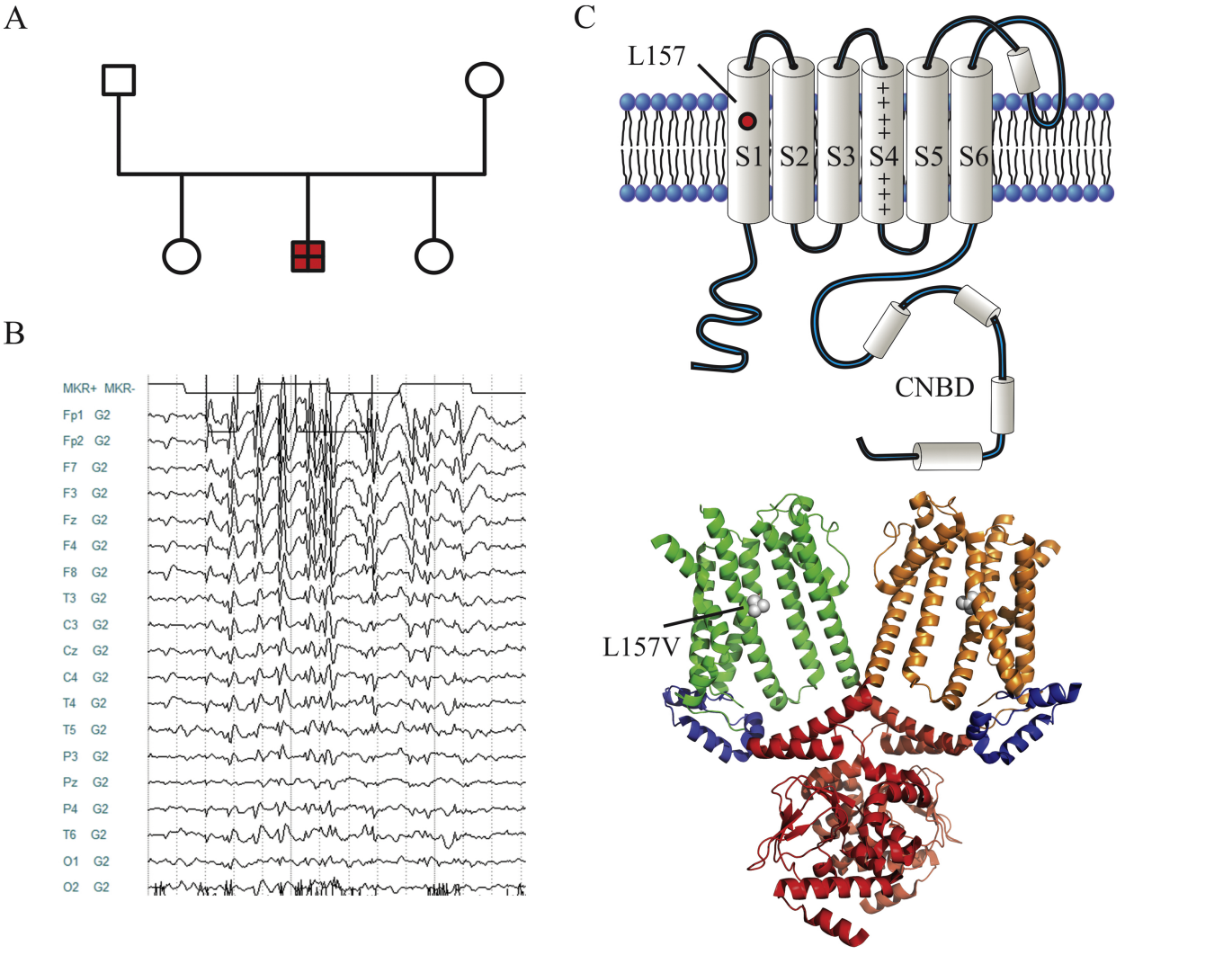
A
B
MKR+ MKR-
Fp1 G2
Fp2 G2
F7 G2
F3 G2
Fz G2
F4 G2
F8 G2
T3 G2
C3 G2
Cz G2
C4 G2
T4 G2
T5 G2
P3 G2
Pz G2
P4 G2
T6 G2
O1 G2
O2 G2
C
L157
S1
S2
S3
S4
S5
S6
CNBD
L157V
D
S1
S2
hHCN4 259 SDFRFYWDLTMLLLMVGNLIIIPVGITFFKDENTTPWIVFNVVSDTFFLIDLVLNFRTG 317
hHCN3 90 SDFRFYWDLIMLLLMVGNLIVLPVGITFFKEENSPPWIVFNVLSDTFFLLDLVLNFRTG 148
hHCN2 208 SDFRFYWDFTMLLFMVGNLIIIPVGITFFKDETTAPWIVFNVVSDTFFLMDLVLNFRTG 266
hHCN1 139 SDFRFYWDLIMLIMMVGNLVIIPVGITFFTEQTTTPWIIFNVASDTVFLLDLIMNFRTG 197

Figure 1

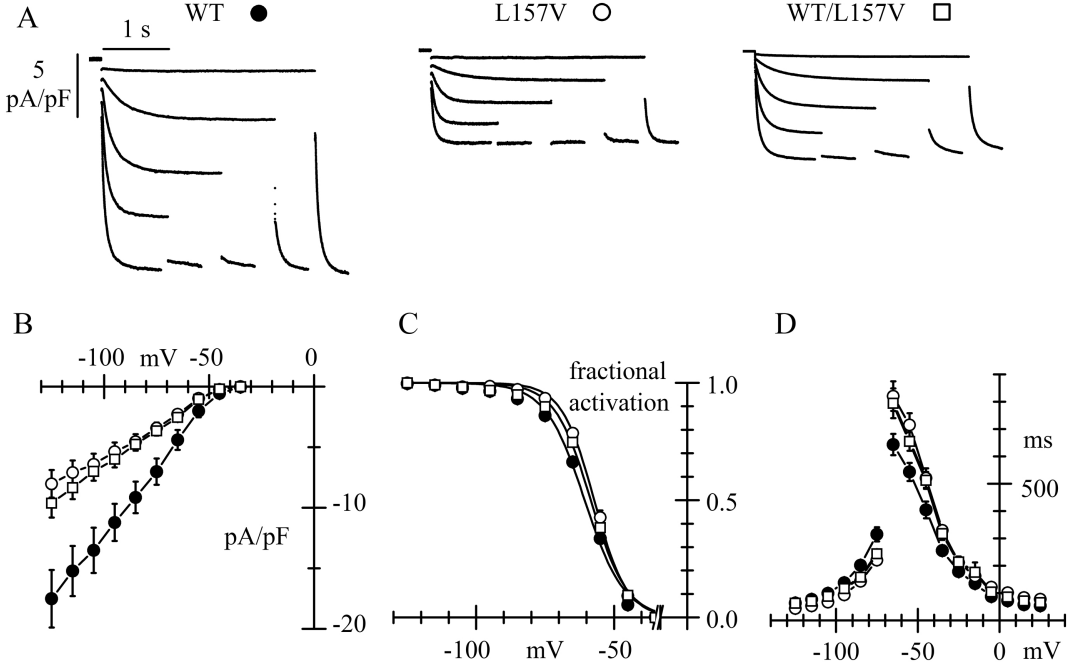
A
1 s
WT
L157V
WT/L157V
5
pA/pF
B
-100 mV -50 0
-10
-20
pA/pF
C
fractional
activation
1.0
0.5
0.0
-100 mV -50
D
ms
500
-100 -50 0 mV

Figure 2

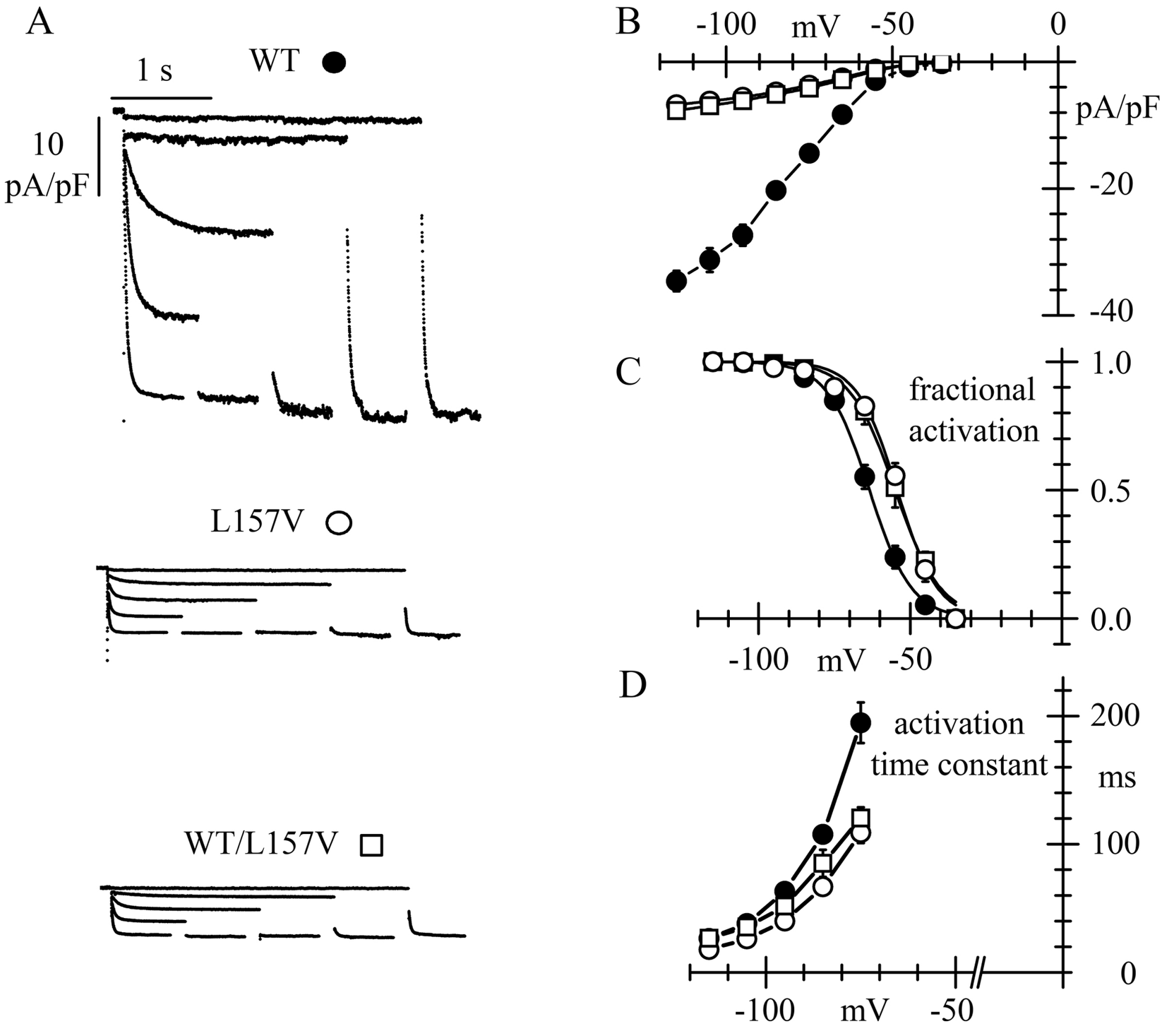
A
1 s
WT
10
pA/pF
L157V
WT/L157V
B
-100
mV
-50
0
pA/pF
-20
-40
C
fractional
activation
1.0
0.5
0.0
-100
mV
-50
D
activation
time constant
200
ms
100
0
-100
mV
-50

Figure 3

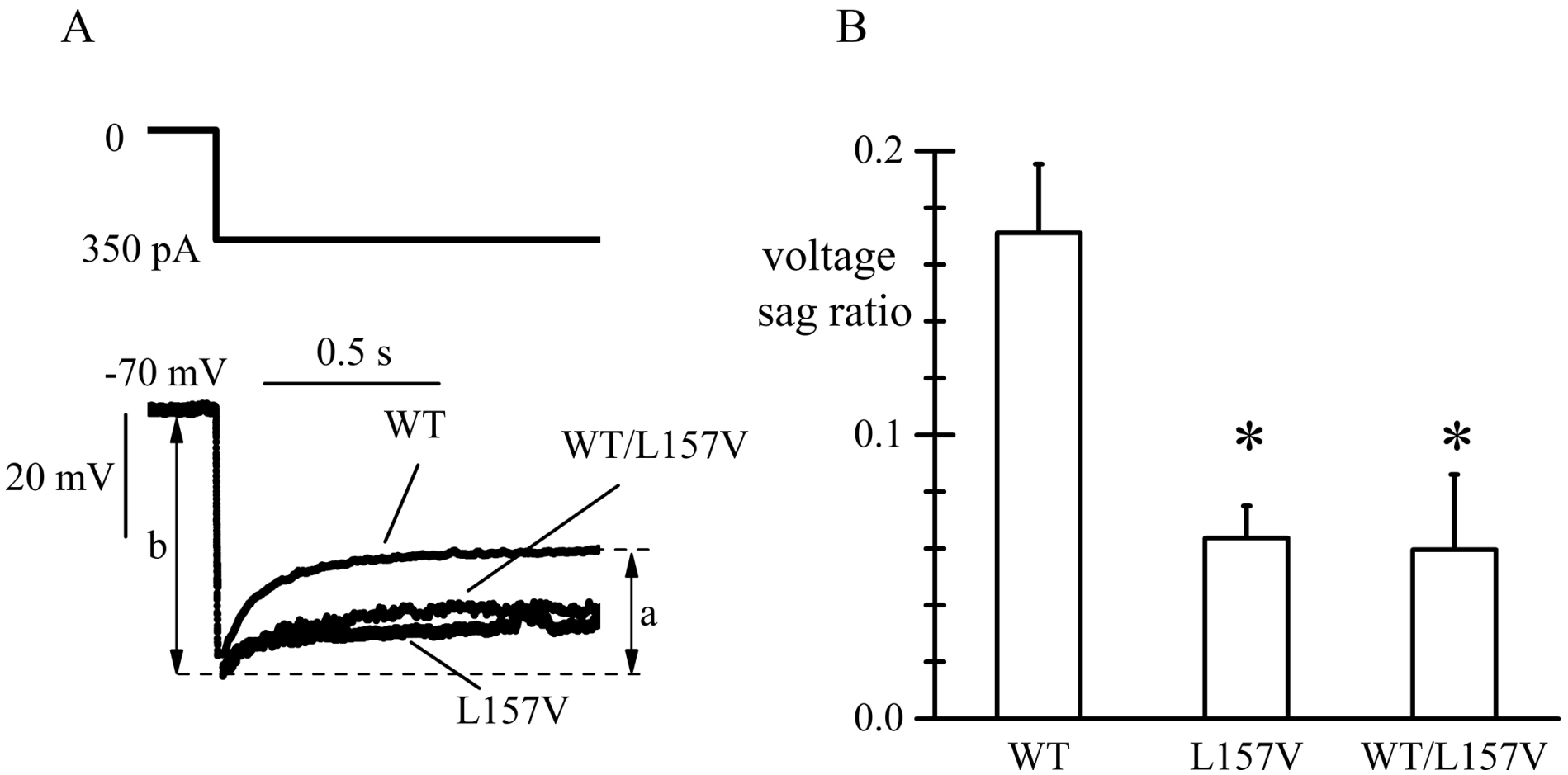
A
0
350 pA
-70 mV
0.5 s
WT
WT/L157V
20 mV
b
a
L157V
B
0.2
voltage
sag ratio
0.1
0.0
*
*
WT
L157V
WT/L157V

Figure 4

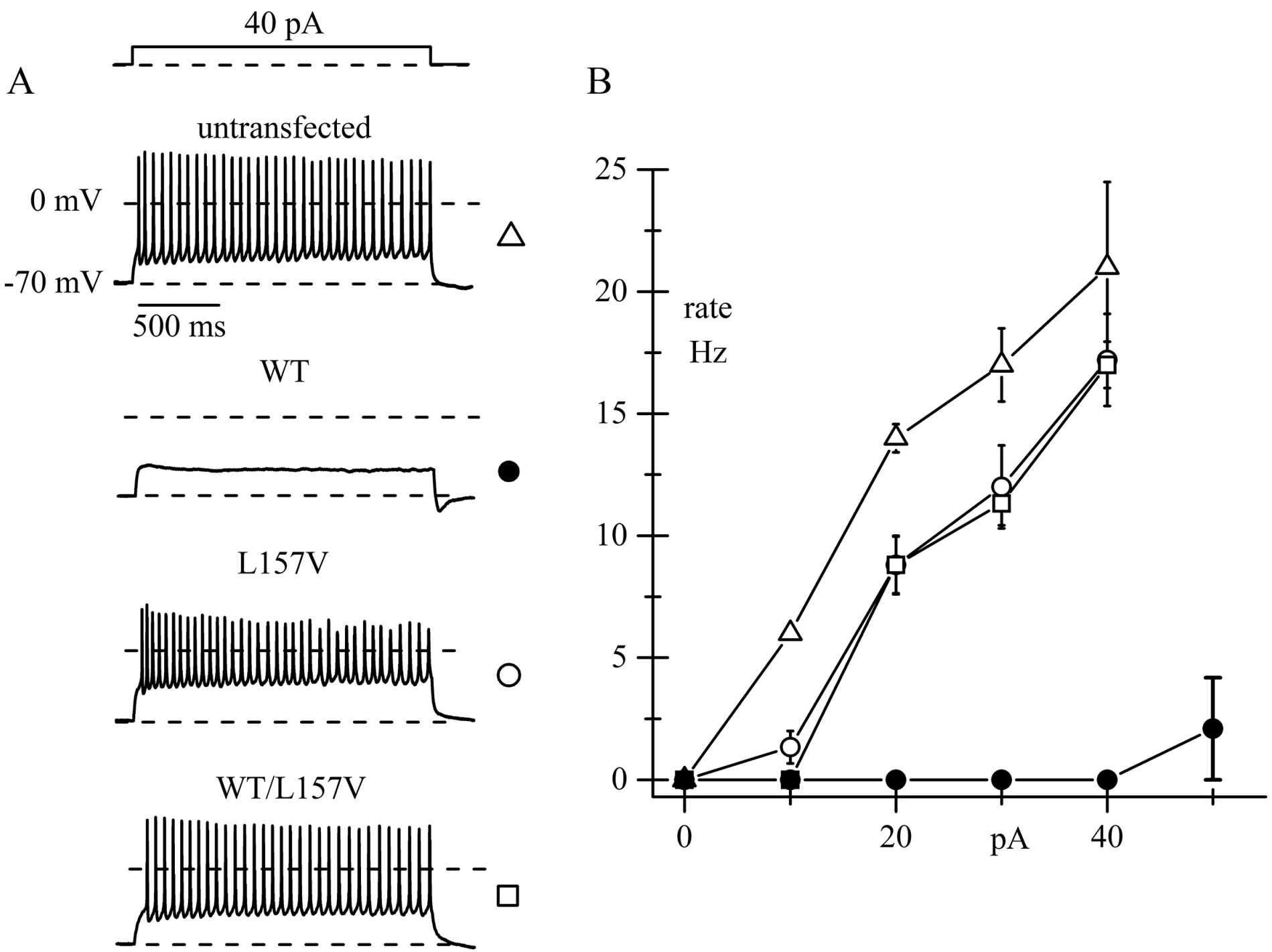
40 pA
A
untransfected
0 mV
-70 mV
500 ms
WT
L157V
WT/L157V
B
25
20
15
10
5
0
rate
Hz
0
20
pA
40

Figure 5

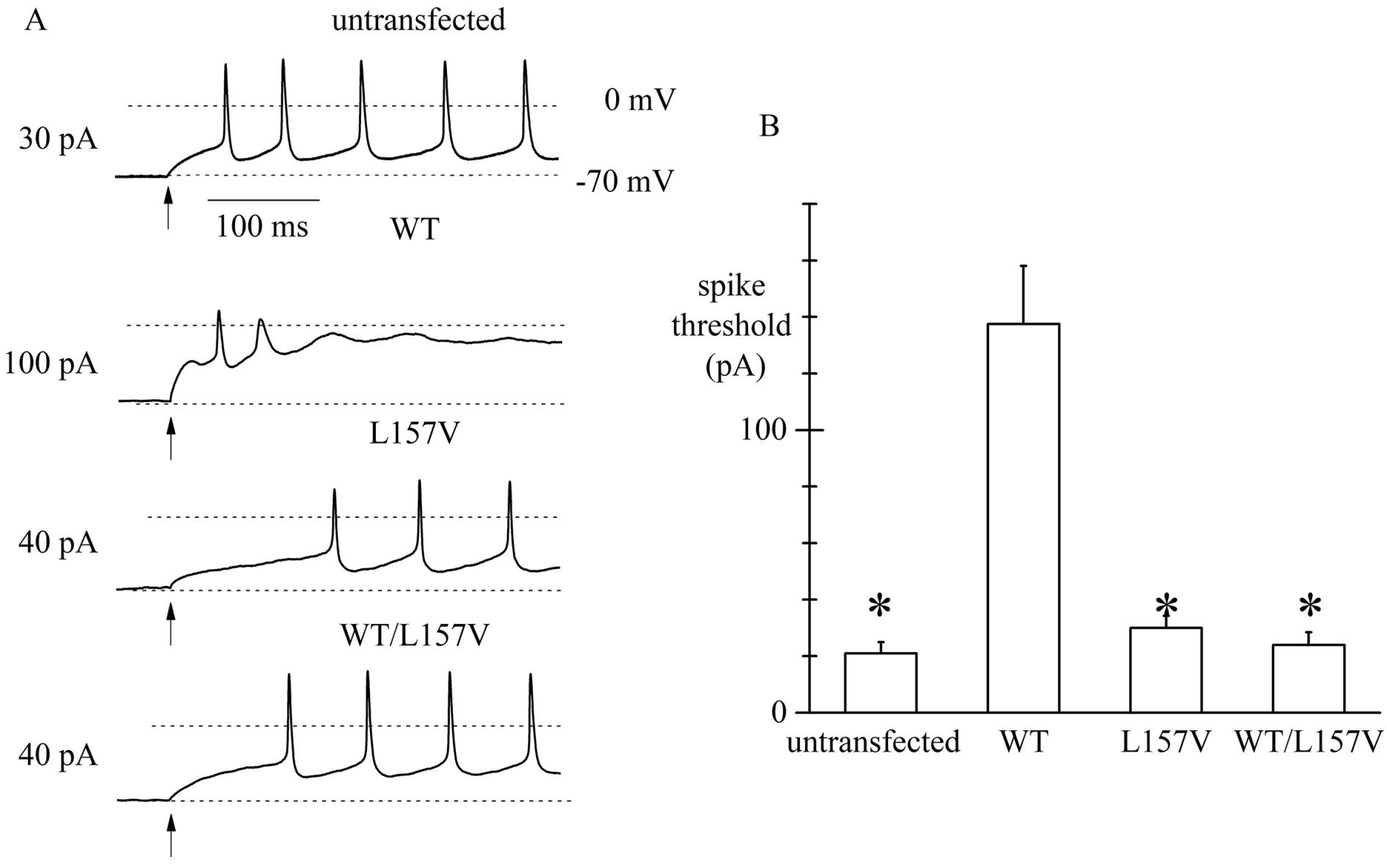
A
untransfected
0 mV
30 pA
-70 mV
100 ms
WT
100 pA
L157V
40 pA
WT/L157V
40 pA
B
spike
threshold
(pA)
100
0
*
*
*
untransfected
WT
L157V
WT/L157V

Figure 6